Journal of Ocean Engineering and Marine Energy (2020) 6:211–220
https://doi.org/10.1007/s40722-020-00162-y

CASE STUDY

A CFD analysis of NREL's 5MW wind turbine in full and model scales

Mariana L. Pinto[1] · **Guilherme R. Franzini**[1] · **Alexandre N. Simos**[1]

Received: 6 June 2019 / Accepted: 4 April 2020 / Published online: 8 May 2020

Abstract
In the present paper, a commercial CFD code based on RANS equations is used to assess the aerodynamic behavior of the rotor of NREL's 5MW turbine. The main objective is to evaluate the changes that happen in the wind flow when the scale of the problem is reduced based on Froude-scale law, a procedure that is used for tests of floating wind turbines in wave basins, such as the ones performed as part of the OC4 program. Therefore, the CFD simulations are performed both for real and model scales, considering a range of tip-speed ratios, and the scale effects involved in the aerodynamics of the blades are presented and discussed. The results are compared to experimental and numerical data of the same rotor available in the literature, especially in terms of thrust and power coefficients. As main conclusions, it is found that the present CFD predictions for the rotor in full scale are generally in accordance with the previous numerical data. More importantly, for the model-scale rotor, it is shown that a very good agreement with the experimental data could be obtained, even for the negative power coefficients that happen for certain tip-speed ratios, something that the previous numerical works have reported to be more difficult to reproduce.

Keywords FOWT · Rotor aerodynamics · CFD modelling · Scale effects

1 Introduction

In the last decades, wind energy has been significantly growing and has consolidated its position as one of the main alternatives for large-scale clean energy production (Ohlenforst et al. 2019). By now, onshore and fixed offshore wind turbines are commonly employed and, more recently, the floating offshore wind turbines (FOWTs) showed that, in various demonstration projects, they can also be economically attractive (WindEurope 2017; Arapogianni et al. 2013).

Compared to the fixed turbines, the FOWT rotor dynamics is more complex mainly because of the floater motions induced by waves and their interactions with the mooring system (Matha et al. 2011). For a proper dynamic analysis of the FOWT, the designer must rely on numerical models that are capable to deal with the complex dynamics and its many couplings (Cordle and Jonkman 2011). Computational tools based on BEMT, such as FAST (Moriarty and Hansen 2005), are generally used to predict the performance of FOWTs. These tools are fast and accurate enough for design purposes, but do not take into account a more refined description of the flow around the blades and in their wake, something that may be important for more specific analysis regarding the blade elasticity and pitch control, for example.

Also, following the standard already adopted for other kinds of floating offshore systems, a number of model-scale experiments have been performed in the FOWT analysis (Martin et al. 2014; Ridder et al. 2014; Kim and Shin 2016; Kim et al. 2019; Sarmiento et al. 2019), as a means for calibrating and/or verifying the numerical models. In this respect, Martin et al. (2014) performed a Froude-scale-based testing of the OC4 semi-submersible FOWT, where a 1:50 scaled model of the NREL 5MW wind turbine has been used. Nonetheless, the scale reduction of the FOWT for testing in waves imposes severe scale effects. For guaranteeing the similarity of the wave effects, the Froude-scaling laws must be applied, whereas the aerodynamics of the blades is ruled by the Reynolds-scaling laws. For practical reasons, it is impossible to achieve Reynolds and Froude similitude simultaneously. Therefore, in experiments where the model is subjected simultaneously to significant loads from wind and waves, the choice of the scaling method becomes a challenge. For testing the FOWTs in a wave basin, tests adopt Froude

✉ Mariana L. Pinto
marianalopes@usp.br

[1] University of Sao Paulo, Av. Prof. Mello Moraes 2230, São Paulo, Brazil

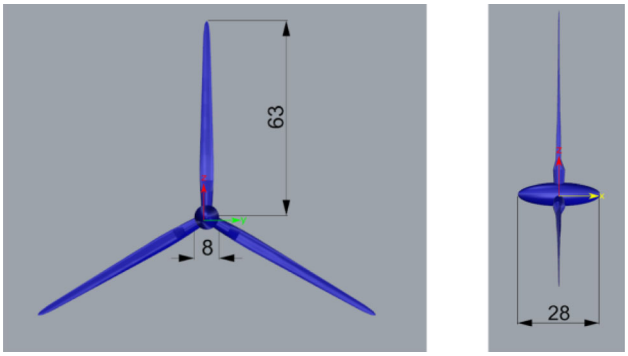

Fig. 1 NREL 5MW baseline rotor geometry. Front view (left) and side view (right)

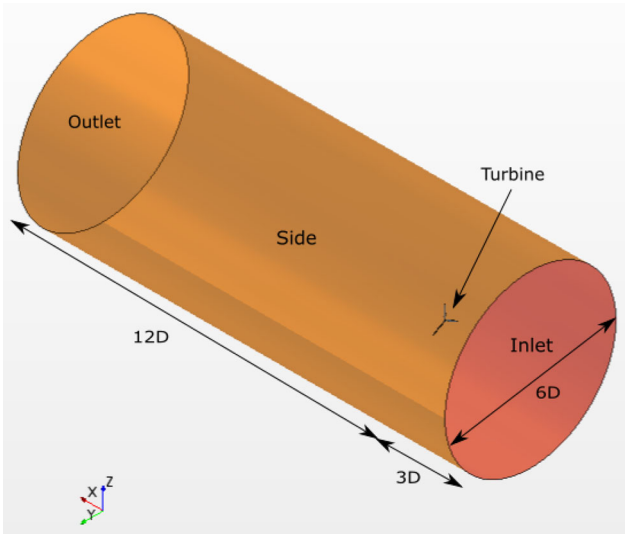

Fig. 2 Sketch of the numerical domain

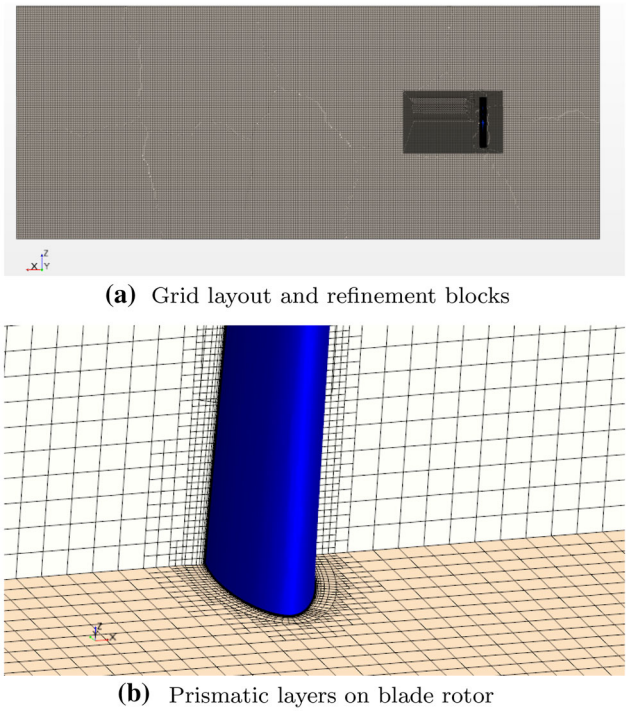

(a) Grid layout and refinement blocks

(b) Prismatic layers on blade rotor

Fig. 3 Grid layout and details

similitude and a scale factor that typically range from 40 to 100, depending on the physical and operating constraints of the particular facility, such as the size of the tank, the limits of the wavemaking system and those of the wind generator.

Due to the much smaller Reynolds number of the wind flow, the flow around the model blades and in their wake can be quite different from the one in prototype scale, which, in its turn, leads to a poor performance of the model-scale turbine. Therefore, to design (and maybe improve, in the future) this kind of model-scale experiments, it is important to fully understand the physics of the flow in the different scales and to be able to predict quantitatively the effects of the scale reduction. For this, CFD modeling is an obvious alternative.

Several studies that deal with CFD modelling of FOWTs have been published. Zhao et al. (2014) performed CFD calculations in full scale for different wind velocities and constant rotor rotation to investigate the aerodynamic performances of NREL 5MW rotor. The turbine tower and floater motions are not considered. In OpenFOAM code, the steady RANS equations with $k-\omega$ SST turbulence model and multiple reference frame for the rotational motion are solved. The CFD results show good agreement with the ones obtained from FAST simulation under the same conditions.

Giahi and Dehkordi (2016) investigated how the experience gained concerning the influence of scaling on wind turbines can be used for moving from the design of a smaller turbine to the design of a larger one. The CFD results are in excellent agreement with predictions of Similarity Theory,

Table 1 Properties of NREL 5MW turbine in full and model scale

Properties	Full scale	Model scale	Unit
Rated power	5	5.70	(MW)/(W)
Rotor diameter	126	2:52	(m)
Hub height (above sea level)	90	1.80	(m)
Wind speed nominal	11.4	1.60	(m / s)
Reynolds (0.7 rotor radius)	1.15×10^7	3.57×10^4	(–)

Table 2 Environmental conditions in full and model scales

Scale	Wind velocity (m/s)	TSR	Ω (rad/s)
Full	11.4	3	0.54
Full	11.4	4	0.72
Full	11.4	5	0.90
Full	11.4	6	1.09
Full	11.4	7	1.27
Model	1.61	3	3.84
Model	1.61	4	5.12
Model	1.61	5	6.40
Model	1.61	6	7.68
Model	1.61	7	8.96

except for low velocities, when the flow pattern is different in each scale.

Make and Vaz (2015) investigated the aerodynamic behavior of two wind turbines (NREL 5MW and MWST) using CFD calculations in model and full scale for different tip-speed ratios, varying angular velocity for a constant wind velocity. Also, the tower and floater motions are not considered. The steady RANS equations with $k-\omega$ SST turbulence model are applied. The numerical results which they report are in good agreement with experimental data, except the ones regarding the power coefficient of the NREL turbine in model scale, for which the trend of variation with tip-speed ratio is opposite with respect to the one derived from the experimental measurements. In addition, Make and Vaz (2015) presents a discussion on the scale effects, showing that, as expected, the flow pattern around the blades was quite affected by them, leading to power and thrust curves that are very different in model and full scale.

Wu et al. (2015) developed a CFD model for simulating the aerodynamics of the full-scale NREL 5MW rotor subjected to pitch motion of the floater. Liu et al. (2016) has also investigated the effect of 3 degrees of freedom (DoF) motions (surge, heave, and pitch) on the aerodynamic performance of a floating wind turbine rotor.

Simulations considering all the degrees of freedom involved in the problem or/and the complete geometry of the floating wind turbine (rotor, tower, and floater) are still a challenge, especially due to their high computational costs. Liu et al. (2017) modeled a complete FOWT with 3DoF to analyze the motion response of the floater and aerodynamic forces of the turbine in wind and waves. However, only two environmental conditions are analyzed due to the high computational costs.

Zhou et al. (2019) also investigated a complete FOWT with 3DoF, but the objective was to assess the hydrodynamic and structural dynamic response of the system and there are no data regarding the aerodynamic forces. Moreover, Cheng et al. (2019) carried out CFD calculations including 6DoF of the floater, and the turbine rotor is modeled as an actuator disk. Although a coarse mesh is employed, the results are in line with the other references.

In the present paper, a commercial CFD, StarCCM+ (CD-Adapco 2019), code based on unsteady Reynolds-averaged Navier–Stokes (URANS) has been applied to predict the performance of the rotor of the 5MW NREL wind turbine, both in full scale and in the same model scale adopted in Make and Vaz (2015) (scale factor of 1:50). The main objective was to evaluate the differences of the flow around the rotor and to understand how they affected the aerodynamic performance coefficients in both scales. For that, the computations were carried out for different tip-speed ratios (TSR), which were changed by varying the rotor angular speed for a constant and uniform incident wind speed. It is important to emphasize that only the rotor geometry was modelled in this stage, and all the computations were done considering that the rotor

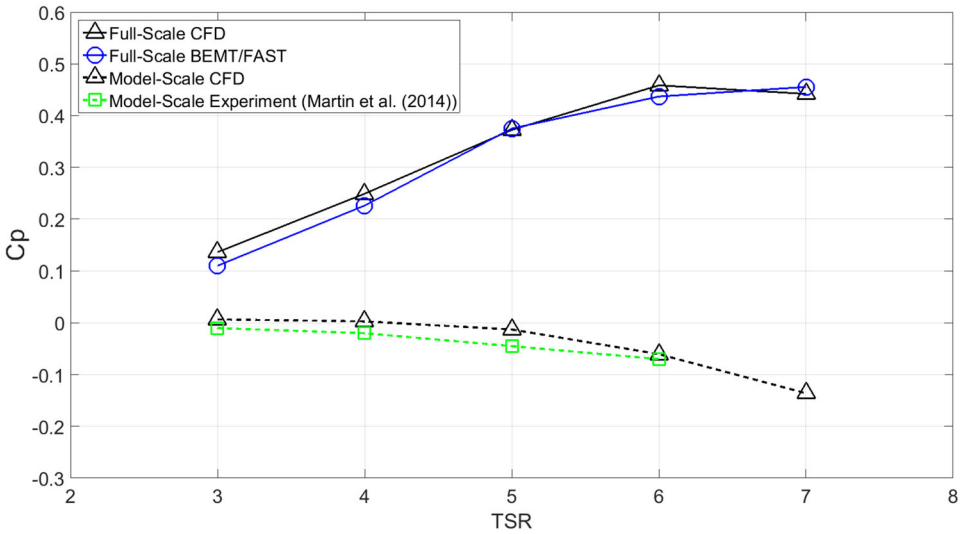

Fig. 4 Power coefficients in model and full scales

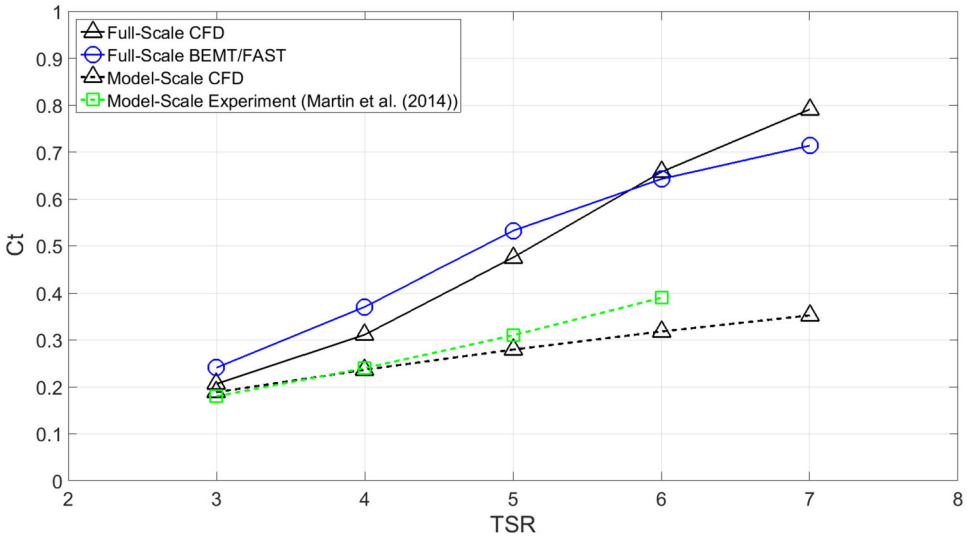

Fig. 5 Thrust coefficients in model and full scales

axis was fixed, thus not taking into account any motions of the floater.

The main features adopted in the numerical model are presented in the next section, followed by the comparison of the results with the experimental ones previously reported in the literature.

2 Numerical model

The governing equations for a transient, unsteady, incompressible and viscous fluid flow are continuity and unsteady Reynolds-averaged Navier–Stokes (URANS). A $k-\omega$ shear stress transport (SST) turbulence model is applied ($k = \frac{3}{2}(\mathbf{I}v)^2$ e $\omega = \frac{\rho k}{(\mu_t/\mu)\mu}$, where v is the incident wind velocity and $\mu_t/\mu = 10$). The equations are discretized using the finite volume method and solved in a segregated scheme; the PIMPLE algorithm is applied to correct the pressure–velocity. A second-order upwind scheme is used for the discretization of convective terms, whereas a second-order central scheme is used for the diffusive flux. A second-order time discretization is also used.

The rotor of the NREL 5MW turbine is modeled according to Jonkman et al. (2009). Figure 1 shows the three-bladed rotor geometry. The rotor diameter is $D = 126$ m and, as can be seen in the figure, an ellipsoidal hub was adopted. Neither the nacelle geometry nor the tower are considered in the numerical model. In this way, absolute formulation (AFM) could be used to describe the rotational motion of the turbine, meaning that the equations are solved in the moving (rotating) reference frame but written in terms of inertial reference frame quantities.

The numerical domain consists of a circular cylinder with a diameter of 6D and a length of 15D, Fig. 2; the turbine is positioned at a distance of 1/5 of the length measured from the

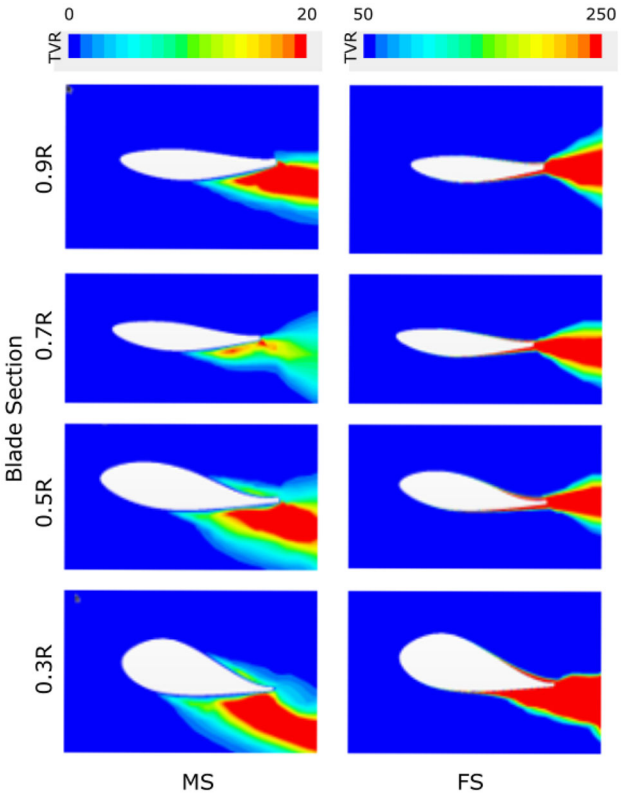

Fig. 6 Turbulence viscosity ratio (TVR) in model scale (left) and full scale (right) in different blade section

inlet, dimensions adopted according to the ones suggested by Wu et al. (2015) and Giahi and Dehkordi (2016). The domain boundaries are defined by uniform inlet velocity, pressure outlet, and constant pressure in the far-field and non-slip surface on the rotor body (Table 1).

The computational grids are generated using hexahedral elements and prismatic layers are applied on the rotor

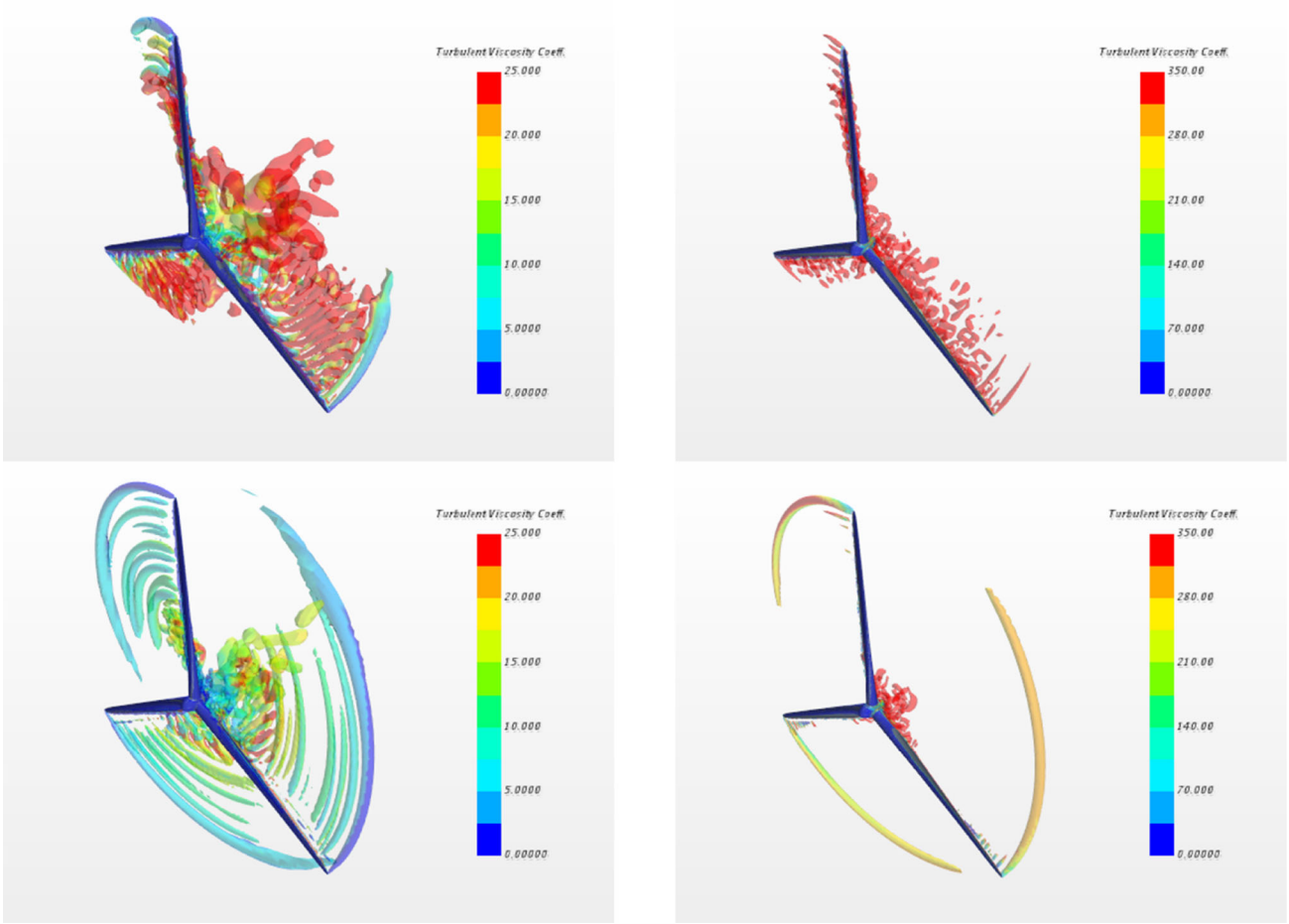

Fig. 7 Turbulence viscosity ratio in model (left) and full (right) scales for TSR = 3 (above) and TSR = 7 (below) on a Q-criterion surface ($Q = 5$)

surface; Fig. 3 shows a typical grid layout. All grids are generated, such that $y_+ \approx 1$ with cell growth in the wall normal direction of 1.20. This is done to avoid the use of wall functions and to properly model the flow in the immediate vicinity of the body surface, which is of utmost importance for the low Reynolds numbers. Two refinement blocks are applied near the rotor, which contain the regions of greatest details. The grids have 28 million elements.

The time-step adopted in the simulations is equal to a rotation interval of 1° in the TSR = 7 condition. The residuals are typically of order 10^{-6} in all simulations.

To investigate the aerodynamic behavior of the rotor, the incident wind speed is kept constant in time, uniform, and equal to 11.4 m/s in full scale and 1.61 m/s in model scale (in accordance with the Froude-scaling law), as shown in Table 2. Five angular speeds of rotor are imposed for each scale, resulting in five different tip-speed-ratio (TSR) conditions, which are kept the same in both scales.

3 Results and discussion

The power and thrust coefficients of the rotor derived from the simulations in both scales are shown, respectively, in Figs. 4 and 5.

There are no experimental data available concerning the full-scale performance; therefore, the CFD computations are compared to estimated coefficients based on the FAST code. One can observe in the figures that the results show good agreement for the power coefficient and a reasonable one regarding the thrust coefficient.

For the model-scale performance, there are experimental data available and the aerodynamic coefficients presented in Martin et al. (2014) were taken as a reference. The agreement between numerical predictions and those obtained from the experiments is indeed fairly good both for the thrust and the power coefficients. An interesting trend can be observed here, for the power coefficient in model scale shows a somewhat unexpected behavior. For low TSR, the power coefficient is almost null, while for higher ones, it is negative (meaning that, for those particular combinations of wind and rotor

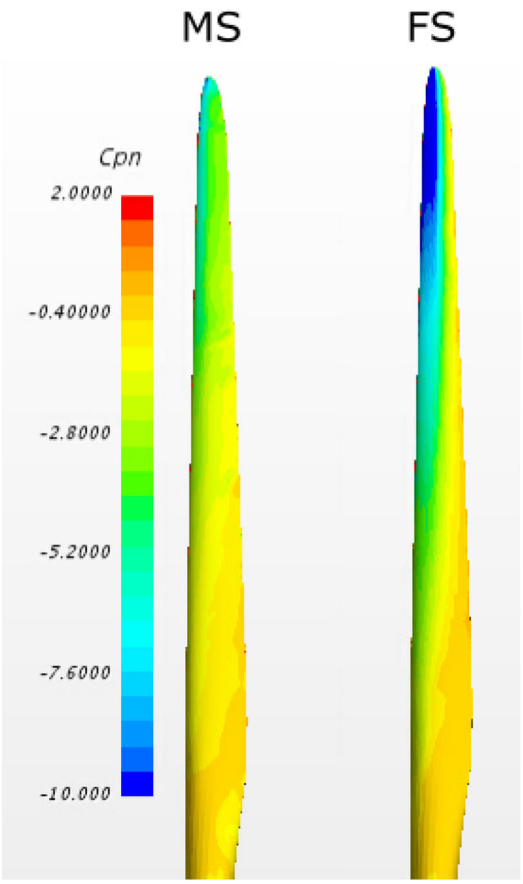

Fig. 8 Pressure coefficient Cpn on the suction side of the blade in model scale (left) and full scale (right)

speed, the rotor is actually supplying power to the flow rather than extracting energy from it).

The performance of the turbine is clearly much poorer in model scale, especially regarding the power, which largely depends on the lift provided by the blades. This happens, because the variation of the Reynolds number of the flow is extremely large: in model scale, the Reynolds number is 10^4, while for the flow in full scale is 10^7. Due to this, the flow around the blades's foils is quite different, something that can be illustrated by the results in Figs. 6 and 7, where the turbulent viscosity ratio in the two scales can be shown over the blades for lowest and highest TSRs. In general, while the boundary layer remains attached to the airfoil in the full scale, with separation occurring only near the trailing edge, in the model scale, the flow detaches much sooner when exposed to larger adverse pressure gradients. As a result, the pressure distribution on the blades is very different, as shown in Fig. 8, where the pressure coefficient on the suction side of a blade is plotted in both scales for some of the TSRs. In model scale, clearly the pressure on the suction side of the blade increases and, as a consequence, the amount of produced power is reduced.

4 Conclusions

In this paper, a commercial CFD code has been applied to investigate the aerodynamic behavior of the rotor of NREL's 5MW turbine in model and full-scale. The CFD results have been compared to numerical (BEMT code—FAST) and experimental data which were available in the literature. The comparison of results for power and thrust coefficients shows good agreement in both scales, attesting that the CFD model was capable of reproducing the scale effects involved in a proper way. Moreover, it is important to highlight that the agreement with the experimental results was particularly good, with the model being able to capture the trends in both the thrust and power coefficients. Indeed, this is not an easy task to accomplish regarding the numerical modeling of the blades, as the previous attempts of Make and Vaz (2015) may attest. The scale effects on the performance of the turbine are very large, and the numerical model shows that the flow on the model blades is generally heavily separated. As a consequence, for the conditions tested, the model rotor experiences around 50% less thrust and provides no significant power. The drop in the thrust is specially important regarding the wave-basin tests, for it also affects the dynamics of the floater and mooring lines. The good performance of the CFD model attests that it is indeed an invaluable tool for predicting the scale effects involved in the wave tests frequently carried out for the FOWTs and certainly one that can be used in the attempt to mitigate them in the future, thus rendering these tests more representative of the real dynamics of the FOWTs in waves. In this respect, new CFD results including prescribed motions of the floater may be a convenient next step in the understanding of the problem. This is, in fact, the approach adopted for instance by Wu et al. (2015). Bolder attempts should not be excluded, of course, including the invaluable efforts to model the whole FOWT in wind and waves, an approach followed, for example, by Zhou et al. (2019), Liu et al. (2017), and Cheng et al. (2019).

Acknowledgements This study was financed in part by the Coordenação de Aperfeiçoamento de Pessoal de Nível Superior, Brasil (CAPES)-Finance Code 001, through the scholarship provided to Mariana Lopes Pinto. Alexandre Nicolaos Simos acknowledges CNPq for his Research Grant. The authors are also in debt to the support received from ONR-Global (Award No N62909-16-1-2066), which enabled the nucleation of the research group on floating wind turbines, in the context of which this research was conducted.

Appendix: Sensitivity analysis

The sensitivity analyses are performed to full and model scale. Domain size, grid refinement, and time step are investigated for the Tip-speed ratio of TSR = 3 and TSR = 7.

Table 3 Domain size sensitivity

Domain ID	Downstream (m)	Upstream (m)	Radial (m)
A	4D	D	2D
B	8D	2D	4D
C	12D	3D	6D

The domain size analysis is carried out to mitigate the effect of boundary conditions on the numerical solution. Three cylindrical domains are investigated (see Fig. 1) and their dimensions are presented in Table 3, as a function of the turbine diameter.

Figure 9 shows the axial velocity coefficient, normalized by incident wind velocity, and blank spaces are regions that difference for incident wind velocity are less than 0.5%. For the smallest domain (especially, TSR = 7), the domain size increases the local velocity near the side boundary.

Table 4 shows the C_t and C_p results, as well the errors relative to the largest domain results, that the influence of boundary conditions is less significant. In the model scale, domain *A* does not converge to TSR = 7, probably by local velocity increasing and the grid does not able to capture the gradients. The influence of domain size is more pronounced in the model scale than in the full scale, due to flow instabilities for this Reynolds number. However, in both scales, C_t and C_p errors tend to decrease with larger domains. Therefore, domain *C* is chosen for all simulations.

Grid sensitivity studies are carried out for five grids, see Table 5. To maintain the geometry as similar as possible between the grids, some procedures are taken. The location of the refinement blocks and the prismatic layers ($y_+ \approx 1$) are kept the same in all grids. The grid quality is ensured; 90% of the elements have cell quality between 0.95 and 1.0, which represents a perfect cubic cell. The refinement blocks are defined as a percentage of the base size, which is 5% of

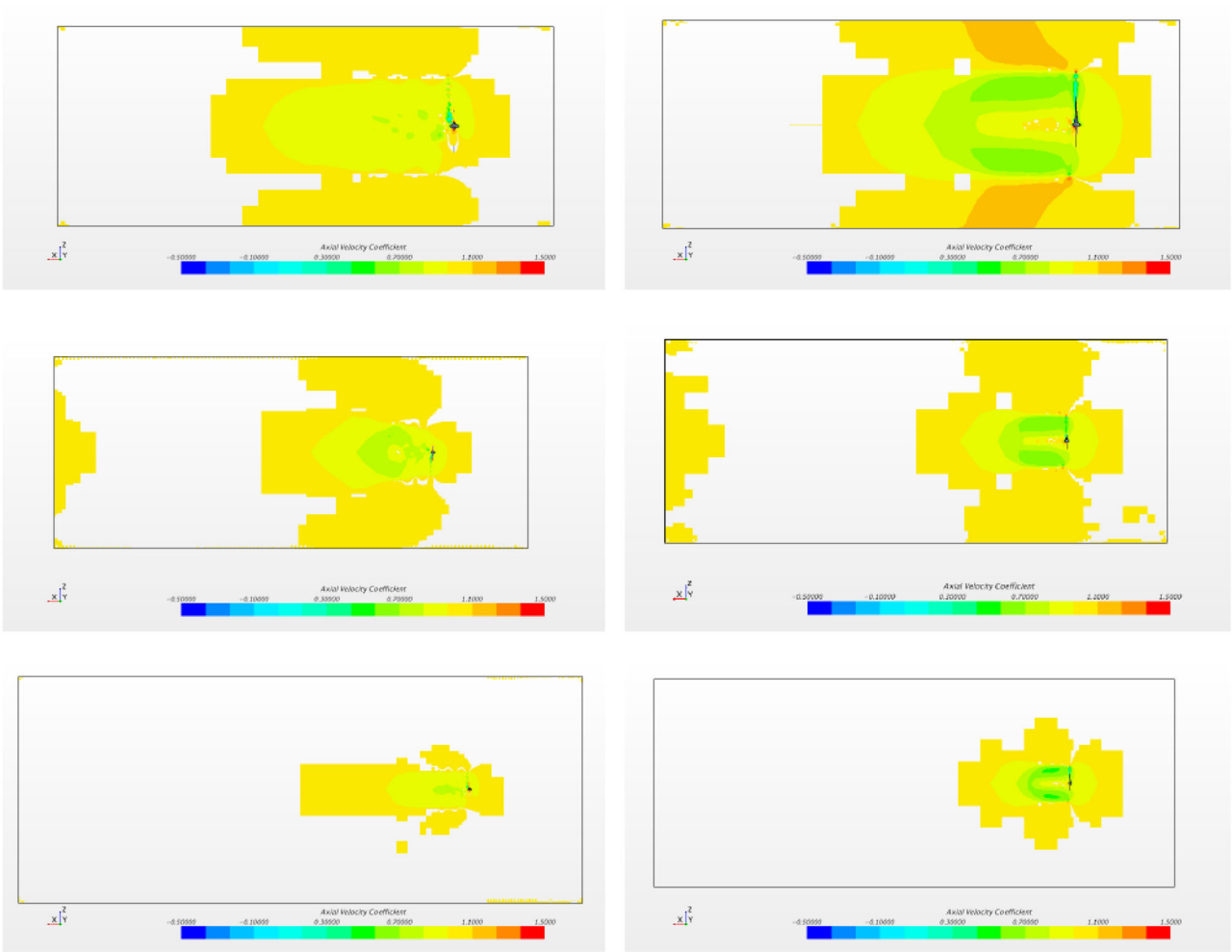

Fig. 9 Axial velocity coefficient in full scale for TSR = 3 (left) and TSR = 7 (right). Domains A (above), domain B (middle), and domain C (below)

Table 4 C_t and C_p results for each domain

Scale	Domain ID	TSR (–)	C_t (–)	C_t error (%)	C_p (–)	C_p error (%)
Full	*A*	3.0	0.2115	1.55	0.1292	1.16
Full	*B*	3.0	0.2063	0.93	0.1290	1.27
Full	*C*	3.0	0.2082	-	0.1307	–
Full	*A*	7.0	0.8523	3.20	0.5372	7.66
Full	*B*	7.0	0.8243	0.19	0.4983	0.13
Full	*C*	7.0	0.8259	-	0.4989	–
Model	*A*	3.0	0.2129	5.48	0.0068	9.27
Model	*B*	3.0	0.2100	4.06	0.0065	5.74
Model	*C*	3.0	0.2018	–	0.0062	–
Model	*A*	7.0	–	–	–	–
Model	*B*	7.0	0.3697	7.71	−0.0829	4.45
Model	*C*	7.0	0.3433	–	−0.0868	–

Table 5 Grid size and CPU time

Scale	Grid ID	Grid size (10^6)	CPU time (h)
Full	*G*	9.82	23.7
Full	*H*	15.21	38.1
Full	*I*	20.50	44.4
Full	*J*	28.70	62.2
Full	*K*	40.35	84.0
Model	*G*	10.05	32.4
Model	*H*	15.98	44.3
Model	*I*	20.77	48.6
Model	*J*	28.84	69.0
Model	*K*	41.45	90.7

Table 6 C_t and C_p for each grid

Scale	Grid ID	TSR (–)	C_t (–)	Error C_t (%)	C_p (–)	Error C_p (%)
Full	*G*	3.0	0.2066	0.10	0.1260	5.40
Full	*H*	3.0	0.2029	1.88	0.1288	3.35
Full	*I*	3.0	0.2039	1.39	0.1285	3.59
Full	*J*	3.0	0.2059	0.40	0.1298	2.54
Full	*K*	3.0	0.2068	–	0.1332	–
Full	*G*	7.0	0.8224	3.51	0.4902	5.43
Full	*H*	7.0	0.8226	3.54	0.4950	6.45
Full	*I*	7.0	0.8142	2.48	0.4754	2.24
Full	*J*	7.0	0.8053	1.36	0.4677	0.59
Full	*K*	7.0	0.7945	–	0.4650	–
Model	*G*	3.0	0.2456	33.77	0.0046	61.28
Model	*H*	3.0	0.2100	14.38	0.0065	45.01
Model	*I*	3.0	0.1919	4.52	0.0110	7.40
Model	*J*	3.0	0.1878	2.30	0.0116	2.75
Model	*K*	3.0	0.1836	–	0.0119	–
Model	*G*	7.0	0.3722	3.45	−0.0723	36.88
Model	*H*	7.0	0.3697	2.77	−0.0829	27.64
Model	*I*	7.0	0.3430	4.68	−0.1059	7.57
Model	*J*	7.0	0.3530	1.90	−0.1115	2.68
Model	*K*	7.0	0.3598	–	−0.1146	–

Table 7 C_t and C_p results for each time-step

Scale	Time ID	TSR (–)	C_t (–)	Erro C_t (%)	C_t (–)	Erro C_t (%)
Full	1.5t	3	0.2070	0.10	0.1401	1.94
Full	t	3	0.2077	0.20	0.1419	0.75
Full	0.5t	3	0.2072	–	0.1429	–
Full	1.5t	7	0.8322	3.49	0.5057	8.08
Full	t	7	0.8053	0.15	0.4677	0.03
Full	0.5t	7	0.8041	–	0.4679	–
Model	1.5t	3	0.1949	3.53	0.0133	14.19
Model	t	3	0.1878	0.21	0.0115	1.16
Model	0.5t	3	0.1882	–	0.0117	–
Model	1.5t	7	0.3745	5.94	−0.1392	24.11
Model	t	7	0.3529	0.15	−0.1115	0.57
Model	0.5t	7	0.3535	–	−0.1122	–

the rotor diameter for the coarse grid. The grids vary between 9 and 41 million of elements and the CPU time[1] for TSR = 7 and four revolutions are given as guide for computational costs.

Table 6 shows the C_t and C_p results for each grid and the errors relative to the finest grid results. The errors decrease with grid refinement. However, the difference between grid J and grid K is small (less than 3% for model-scale), while the computational cost for grid K is 30% higher than grid J. Therefore, grid J (28 million) is chosen.

The initial time-step (t) is equal to a rotation interval of 1 degree in the TSR = 7 condition. Two other time-steps are analyzed, 1.5t and 0.5t. Table 7 shows the C_t and C_p results and the errors relative to the smallest time-step. Significant differences are presented for 1.5t time-step; otherwise, for the initial time-step t, there is a minor difference. Therefore, the initial time-step is appropriated.

References

Arapogianni A, Genachte A, Ochagavia RM, Vergara JP, Castell D (2013) Deep water: the next step for offshore wind energy. European Wind Energy Association (EWEA)

CD-Adapco (2019) Starccm+ users manual. http://www.cd-adapco.com/products/star-ccm/documentation. Accessed on 01 Nov 2019

Cheng P, Huang Y, Wan D (2019) A numerical model for fully coupled aero-hydrodynamic analysis of floating offshore wind turbine. Ocean Eng 173:183–196

Cordle A, Jonkman J (2011) State of the art in floating wind turbine design tools. In: Proceedings of the 21st International Offshore and Polar Engineering Conference, International Offshore and Polar Engineering Conference. Hawaii, USA, pp 367–374

Giahi MH, Dehkordi AJ (2016) Investigating the influence of dimensional scaling on aerodynamic characteristics of wind turbine using CFD simulation. Int J Renew Energy 97:162–168

Jonkman J, Butterfield S, Musial W, Scott G (2009) Definition of a 5-MW reference wind turbine for offshore system development. National Renewable Energy Laboratory

Kim J, Shin H (2016) Model test & numerical simulation of OC4 semi-submersible type floating offshore wind turbine. In: Proceedings of the 26th International Offshore and Polar Engineering Conference, International Society of Offshore and Polar Engineers. Rhodes, Greece, p 6

Kim J, Pham TD, Shin H (2019) Validation of a 750 kW semi-submersible floating offshore wind turbine numerical model with model test data, part II: Model-II. Int J Naval Archit Ocean Eng. https://doi.org/10.1016/j.ijnaoe.2019.07.004

Liu Y, Xiao Q, Incecik A, cheng Wan D (2016) Investigation of the effects of platform motion on the aerodynamics of a floating offshore wind turbine. J Hydrodyn 28(1):95–101

Liu Y, Xiao Q, Incecik A, Peyrard C, Wan D (2017) Establishing a fully coupled CFD analysis tool for floating offshore wind turbines. Int J Renew Energy 112:280–301

Make M, Vaz G (2015) Analyzing scaling effects on offshore wind turbines using CFD. Int J Renew Energy 83:1326–1340

Martin H, Kimball R, Viselli A, Goupee A, (2014) Methodology for Wind/Wave Basin Testing of Floating Offshore Wind Turbine. J Offshore Mech Artic Eng 136(2)

Matha D, Schlipf M, Pereira R, Jonkman J (2011) Challenges in simulation of aerodynamics, hydrodynamics, and mooring-line dynamics of floating offshore wind turbines. In: Proceedings of the 21th International Offshore and Polar Engineering Conference, vol 14. ISOPE, Maui, Hawaii

Moriarty P, Hansen A (2005) Aerodyn Theory Manual. National Renewable Energy Laboratory (NREL)

Ohlenforst K, Sawyer S, Dutton A, Backwell B, Fiestas R, Lee J, Qiao L, Zhao F, Balachandran N (2019) Global Wind Report 2018. Global Wind Energy Council (GWEC)

Ridder E, Otto W, Zondervan G, Huijs F, Vaz G (2014) Development of a scaled-down floating wind turbine for offshore basin testing. In: 33rd International Conference on Ocean, Offshore and Arctic Engineering. ASME, OMAE2014, San Francisco

Sarmiento J, Iturrioz A, Ayllón V, Guanche R, Losada I (2019) Experimental modelling of a multi-use floating platform for wave and wind energy harvesting. Ocean Eng 173:761–773. https://doi.org/10.1016/j.oceaneng.2018.12.046

WindEurope (2017) Floating offshore wind vision statement. WindEurope

[1] 1 core of a Intel(R) Xeon(R) CPU E5-2680 v2 @ 2.80GHz

Wu CH, Vnh-Tan N, Lou J, Sivalingam K (2015) A computacional fluid dynamics model for aerodynamics analysis of offshore wind turbines rotor under floating platform induced motion. In: 34th International Conference on Ocean, Offshore and Arctic Engineering. ASME, OMAE2015, St. John's, Newfoundland

Zhao W, Cheng P, Wan D (2014) Numerical computation of aerodynamic performances of nrel offshore 5-mw baseline wind turbine. In: The Eleventh ISOPE Pacific/Asia Offshore Mechanics Symposium International Society of Offshore and Polar Engineers, Shanghai

Zhou Y, Xiao Q, Liu Y, Incecik A, Peyrard C, Li S, Pan G (2019) Numerical modelling of dynamic responses of a floating offshore wind turbine subject to focused waves. Energies 12(18):3482